Supplementary Material (ESI)

Homochiral Nickel Coordination Polymers Based on Salen(Ni) Metalloligands: Synthesis, Structure and Catalytic Alkene Epoxidation

Yuanbiao Huang, Tianfu Liu, Jingxiang Lin, Jian Lü, Zujin Lin, Rong Cao*

State Key Laboratory of Structural Chemistry, Fujian Institute of Research on the Structure of Matter, The Chinese Academy of Science, Fuzhou 350002, China. E-mail: rcao@fjirsm.ac.cn; Fax: +86 59183796710; Tel: +86 059183796710

Table of Content

16. Figure S13. PXRD patterns of compound **2R** before and after the first catalysis cycle.

17. Scheme S1. Syntheses of ligand *RR*-H_2L and *SS*-H_2L.

18. **Figure S14**. PXRD patterns of compound **6.**

1. **General explanation**

Although PLATON suggests *Pnna* space group for **2R** and **2S** (because the chirality is centered at only two carbon atoms and all heavy scatterers in the unit cell are achiral), the mode of cyclohexyl group is not correct if the *Pnna* is used. And the absolute structure configuration of the homochiral compounds **2R** and **2S** have been further confirmed with the CD spectra. The phenomenon has been found in other homochiral crystals based on the salen ligands (Jeon, Y.; Heo, J.; Mirkin, C. A.; *J. Am. Chem. Soc.* **2007**, *129*, 7480-7481; Li, G.; Yu, W.; Ni, J.; Liu, T.; Liu, Y.; Sheng, E.; Cui, Y. *Angew. Chem. Int. Ed.* **2008**, *47*, 1245–1249; Li, G.; Yu, W.; Cui, Y. *J. Am. Chem. Soc.* **2008**, *130*, 4582-4583; Li, G.; Zhu, C.; Xi, X.; Cui, Y. *Chem. Commun.* **2009**, 2118–2120).

Because of the poorer epoxide yields than the Jacobsen catalyst (Salen(MnCl)), we could not determine the *ee* values of the obtained epoxides.

2. Synthesis of complex *SS*-NiL (1S): The synthesis procedure was similar to that of the complex **1R** except using *SS*-H_2L. The orange crystal of **1S** was grown from the mixture solvent DMF/CH_2Cl_2 (4:3). Anal. Calc. For complex **1S**, $C_{82}H_{98}N_{10}O_6Ni_2$: C, 68.52; H, 6.82; N, 9.75. Found: C, 68.49; H, 6.86; N, 9.79%. IR (KBr, cm^{-1}): 3698 (w), 2949 (m), 2909 (w), 2867 (w), 1678 (w), 1597 (s), 1550 (m), 1532 (w), 1439 (m), 1427 (w), 1411 (m), 1389 (m), 1347 (m), 1324 (w), 1302 (w), 1281 (m), 1264 (w), 1223 (m), 1204 (w), 1174 (m), 1087 (w), 1025 (w), 990 (w), 900 (w), 854 (w), 834 (m), 775 (m), 650 (m).

Synthesis of coordination polymer 2S: The synthesis procedure was similar to that of **2R** except using (*SS*-H_2L) or **1S.** Yield: 63.8 % (based on Ni). Anal. Calc. for **2S**, $C_{93}H_{99}N_9O_9Ni_3$: C, 67.17; H,

6.00; N, 7.58. Found: C, 67.10; H, 6.02; N, 7.61%. IR (KBr, cm^{-1}): 3387 (b), 3069 (w), 3025 (w), 2949 (m), 2865 (w), 1679 (s), 1597 (s), 1551 (m), 1433 (s), 1406 (m), 1385 (m), 1347 (m), 1324 (m), 1281 (m), 1223 (m), 1174 (m) , 1087 (m), 1051 (w), 1025 (w), 991 (w), 899 (w), 834 (w), 820 (w), 787 (w), 650 (m), 575 (w).

Table S1. Selected Bond length (Å) and angles (°) for **1S**, **2R** and **2S**

	1S	**2R**	**2S**
Ni(1)-N(2)	1.841(4)	1.845(3)	1.844(4)
Ni(1)-N(3)	1.842(4)	1.856(3)	1.858(4)
Ni(1)-O(1)	1.854(3)	1.849(3)	1.860(3)
Ni(1)-O(2)	1.830(3)	1.852(3)	1.858(4)
Ni(2)-N(6)	1.849(4)	1.860(3)	1.855(4)
Ni(2)-N(7)	1.842(4)	1.834(3)	1.833(4)
Ni(2)-O(3)	1.849(3)	1.861(3)	1.856(3)
Ni(2)-O(4)	1.847(3)	1.842(3)	1.842(3)
Ni(3)-N(1)	-	2.044(3)	2.045(4)
Ni(3)-O(8)	-	2.189(3)	2.200(4)
Ni(3)-O(7)	-	2.061(3)	2.055(3)
Ni(4)-N(5)	-	2.058(3)	2.059(4)
Ni(4)-O(5)	-	2.193(3)	2.196(4)
Ni(4)-O(6)	-	2.040(3)	2.050(4)
O(1)-Ni(1)-N(3)	93.96(17)	94.23(13)	94.29(16)
O(2)-Ni(1)-N(3)	172.45(15)	176.40(14)	176.42(18)
N(1)-Ni(3)-N(1)#1	-	90.15(18)	89.9(2)
N(1)-Ni(3)-O(8)	-	96.83(12)	96.65(15)

Symmetry transformations used to generate equivalent atoms: #1 (**2R**) -x+1, y, -z+1/2; (**2S**) -x+2, y, -z+3/2.

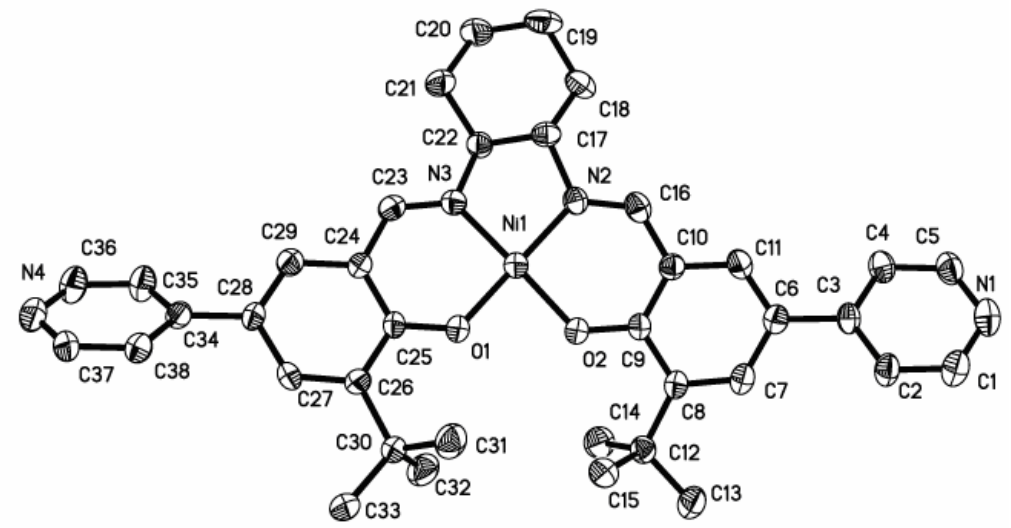
C20
C19
C21
C18
C22
C17
C23
N3
N2
C16
Ni1
C29
C24
C10
C11
C4
C5
C36
N4
C35
C28
C6
C3
N1
C34
C25
O1
O2
C9
C37
C38
C27
C26
C7
C2
C1
C14
C8
C30
C31
C12
C32
C15
C13
C33

(a)

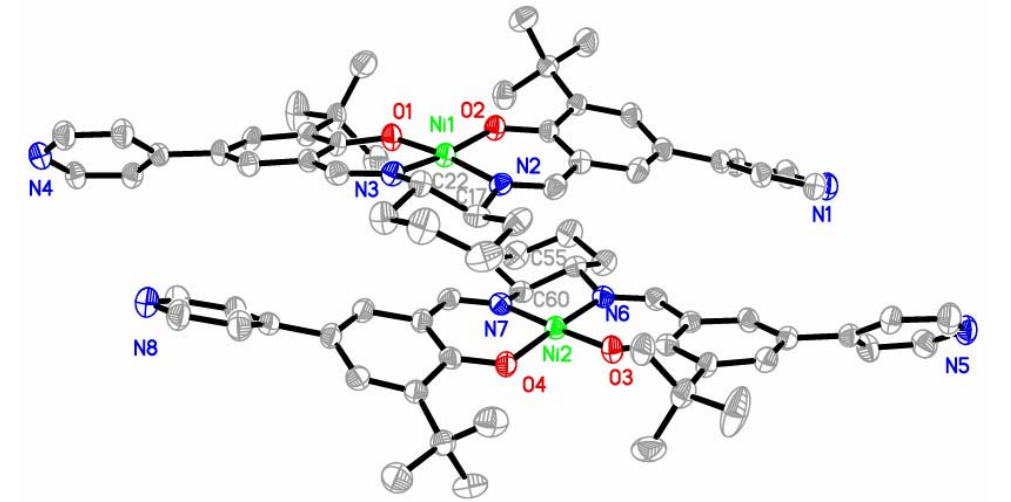
O1
Ni1
O2
N4
N3
N2
N1
C22
C17
C55
C60
N7
N6
N8
Ni2
O4
O3
N5

(b)

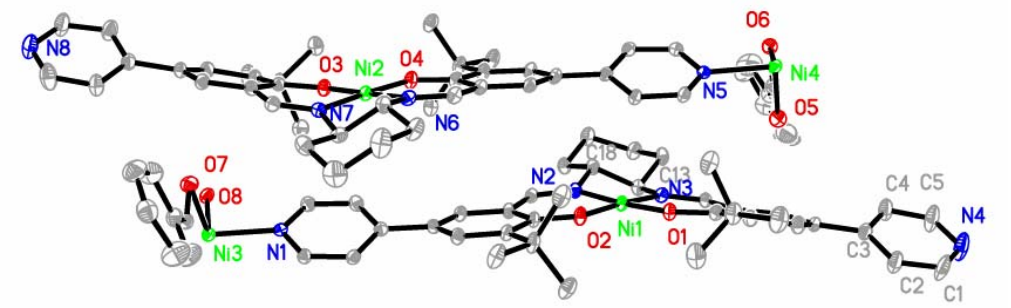
O6
N8
O3
Ni2
O4
Ni4
N5
N7
N6
O5
C18
O7
N2
C13
N3
C4 C5
O8
Ni1
N4
Ni3
N1
O2
O1
C3
C2
C1

(c)

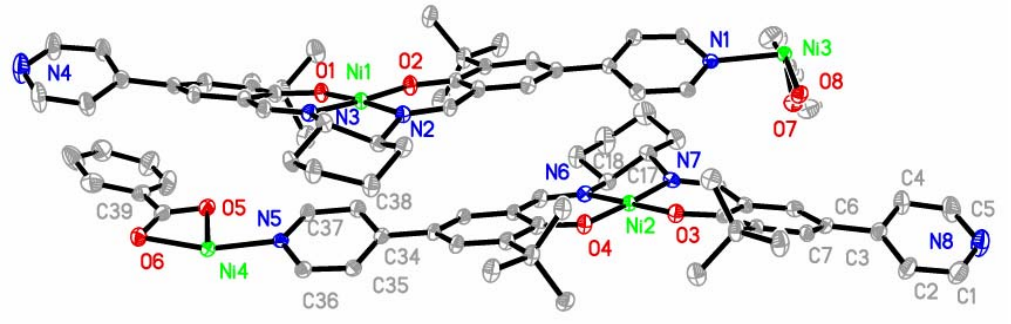

(d)

Figure S1. Asymmetric unit of crystal structures of **1S**(a, b), **2R** (c) and **2S** (d). Hydrogen atoms and solvent molecule DMF are omitted

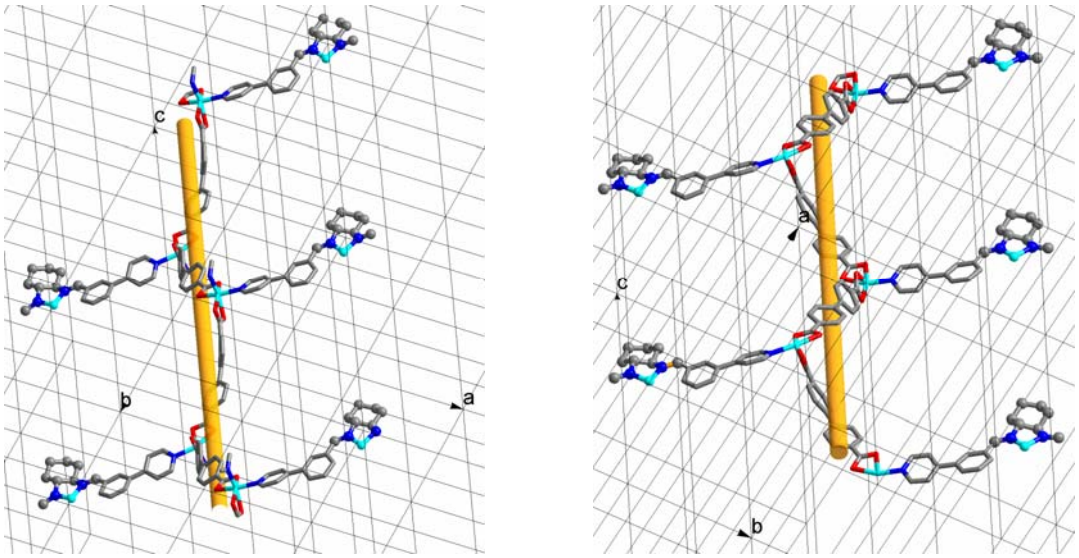

(a) **(b)**

Figure S2. A view of chirality units in the left-handed (a) and right-handed helix polymeric chain of **2R**

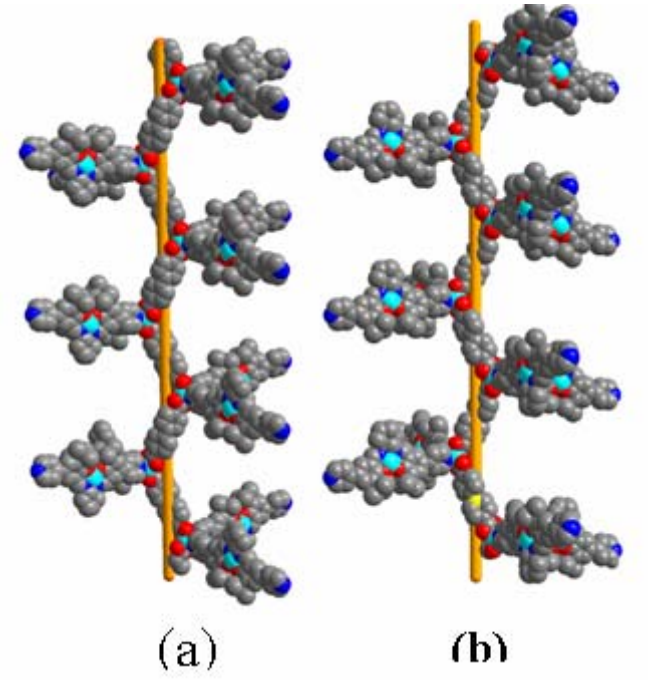

Figure S3. A view of right-handed (a) and left-handed (b) helix polymeric chains in **2S**

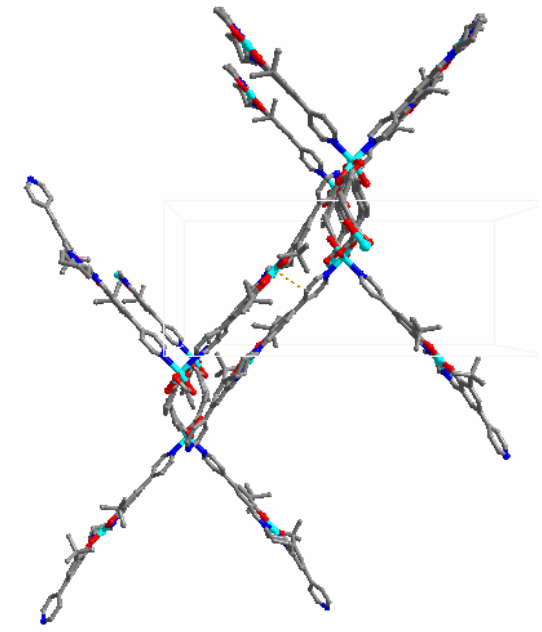

Figure S4. Intermolecular π-π interaction between **2R**

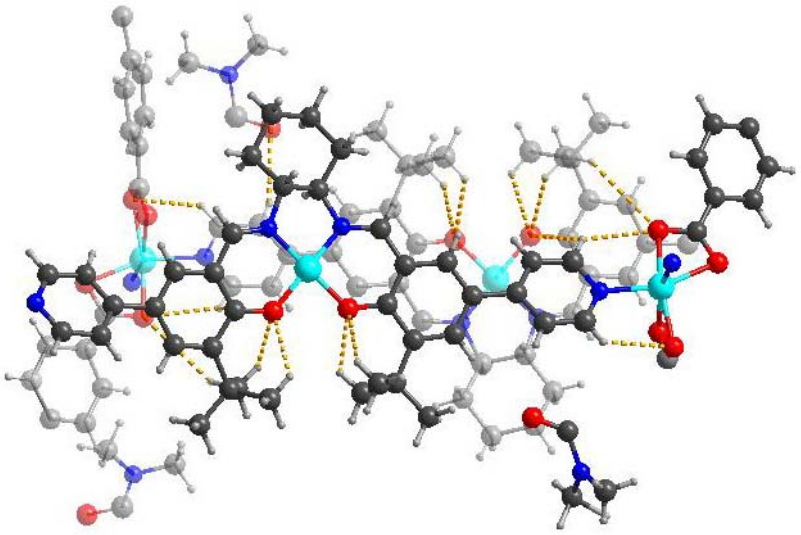

Figure S5. The weak hydrogen bonds in the crystal structure of **2R**

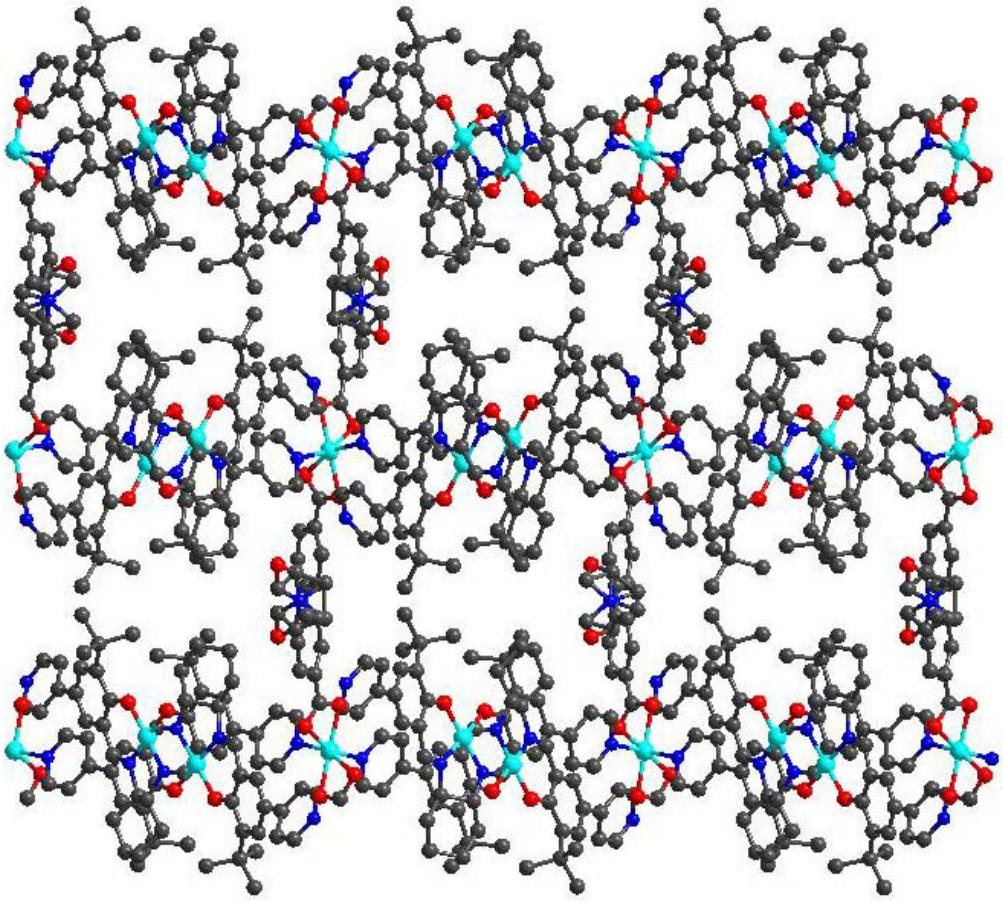

Figure S6. A view of 3D structure of **2R** along the *b*-axis

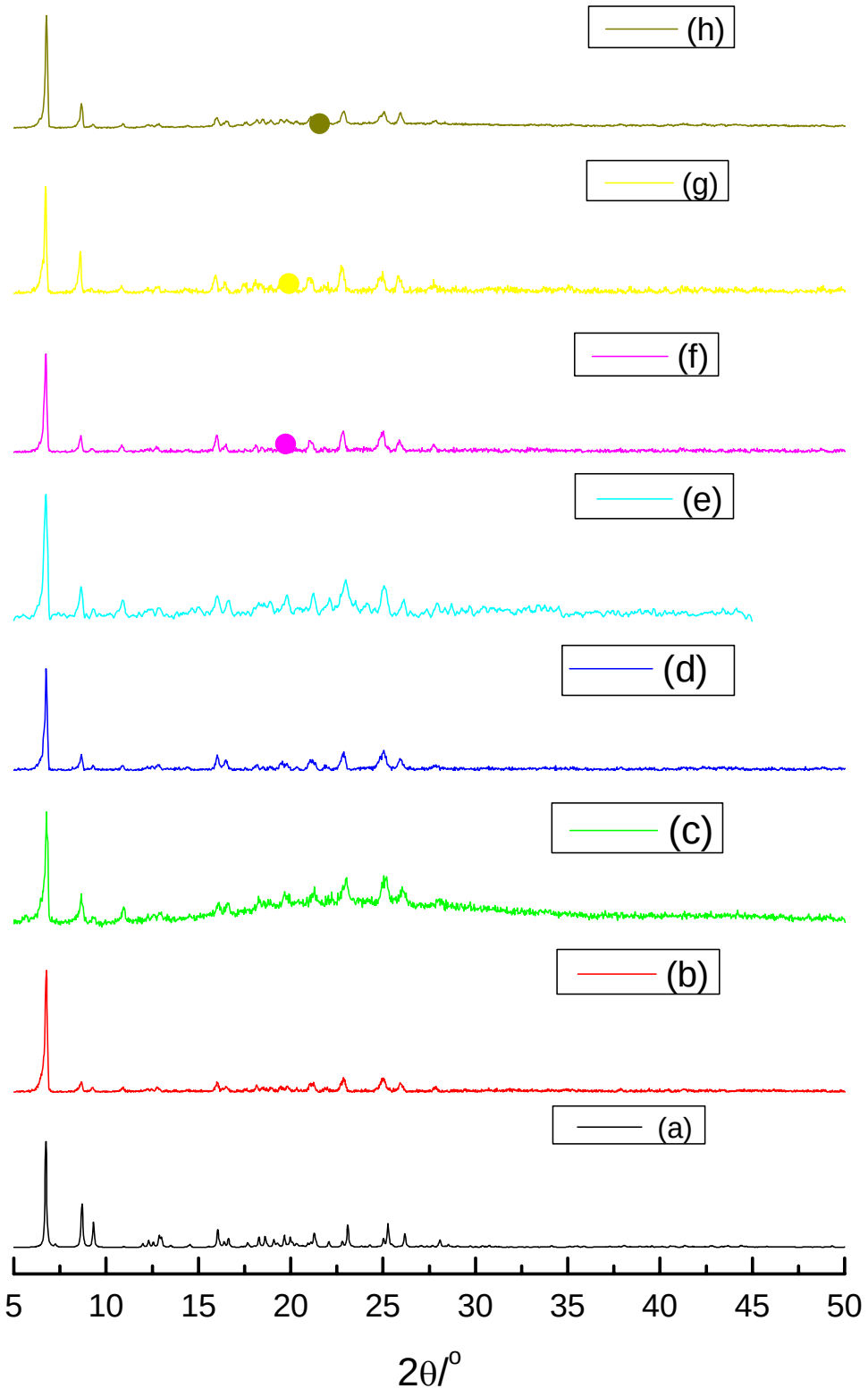

Figure S7. Powder XRD patterns of **2R** and **2S:** (a) simulated compound **2R**; (b) obtained from $Ni(NO_3)_2 \cdot 6H_2O$ and *RR*-H_2L (2:1); (c) obtained from $Ni(NO_3)_2 \cdot 6H_2O$ and *RR*-H_2L (3:1); (d) obtained from $Ni(NO_3)_2 \cdot 6H_2O$ and *RR*-H_2L (4:1); (e) obtained from $NiCl_2 \cdot 6H_2O$ and *RR*-H_2L (2:1); (f) obtained from $Ni(OAc)_2 \cdot 4H_2O$ and *RR*-H_2L (2:1); (g) obtained from $Ni(NO_3)_2 \cdot 6H_2O$ and *RR*-NiL (1:1); (h)

compound **2S** obtained from $Ni(NO_3)_2 \cdot 6H_2O$ and *SS*-H_2L (2:1).

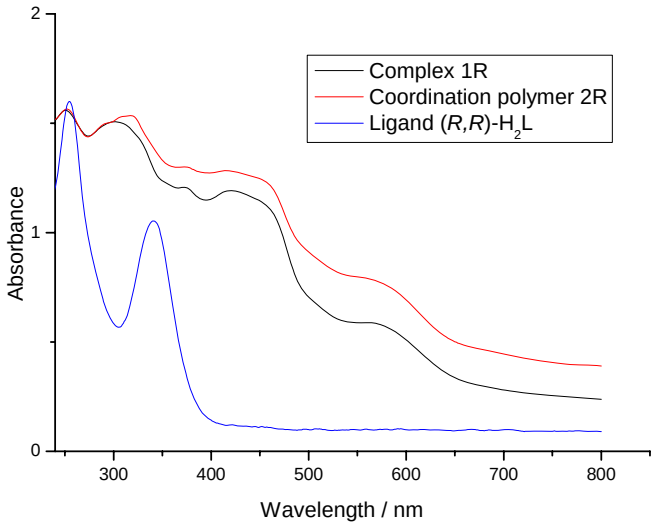

Figure S8. Solid-state UV-Visible absorption spectra of ligand (*R*,*R*)-H_2L and compounds **1R** and **2R**.

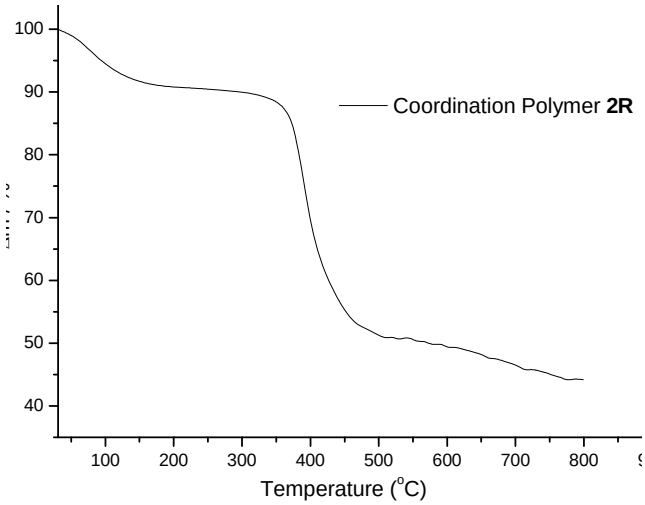

Figure S9. TGA of compound **2R**.

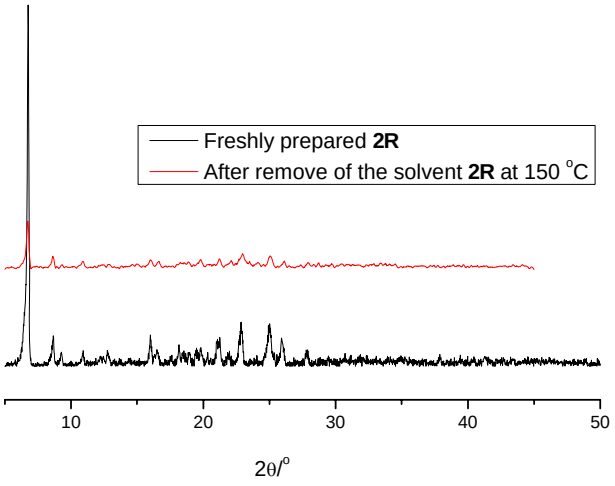

Figure S10. PXRD patterns of compound **2R** before and after removal of the solvent

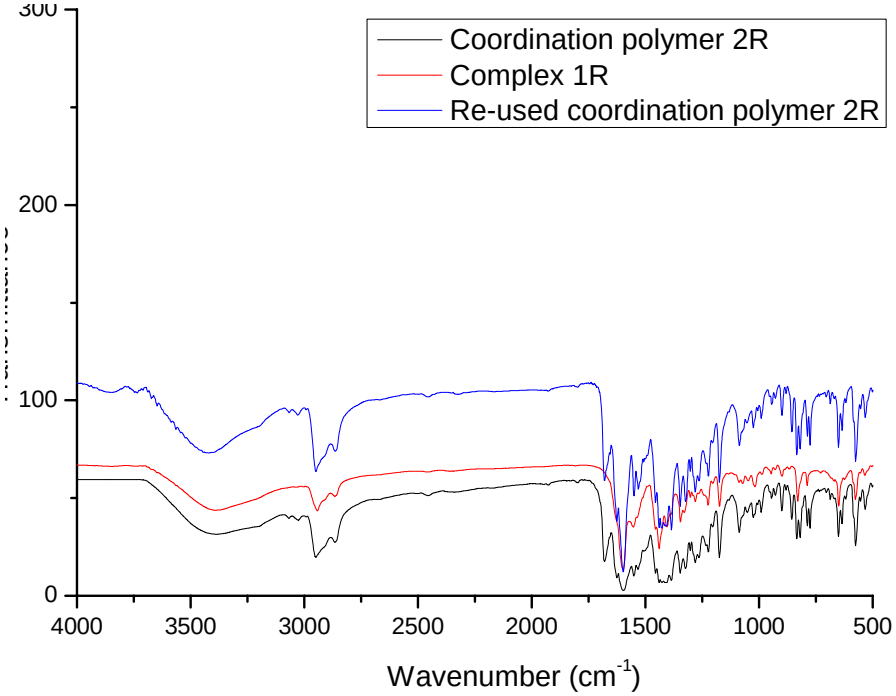

Figure S11. IR of compound **1R** and **2R** before and after the first catalysis cycle

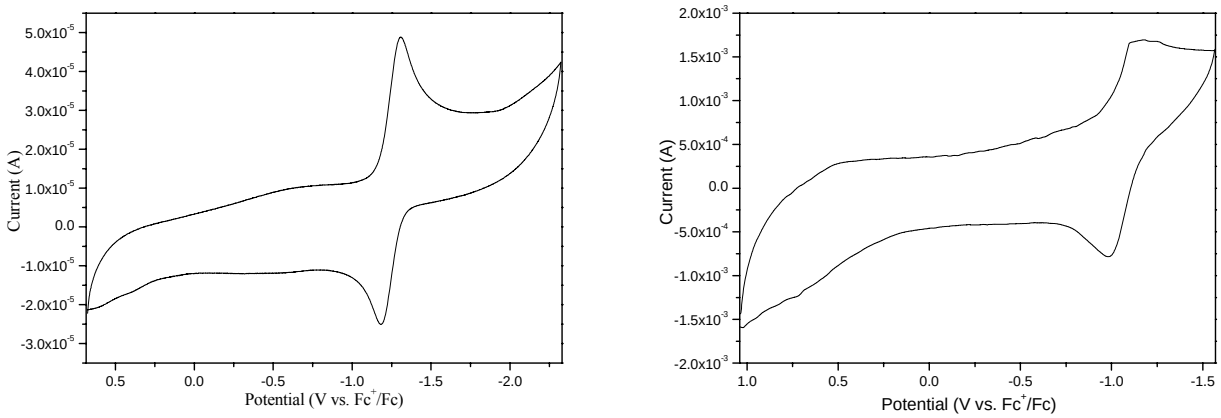

Figure S12. Cyclic voltammograms of **1R** (a) and **2R** (b) in anhydrous DMF (0.1 M N(*n*-Bu)$_4$ClO$_4$) at a scan rate of 50 mV s^{-1}.

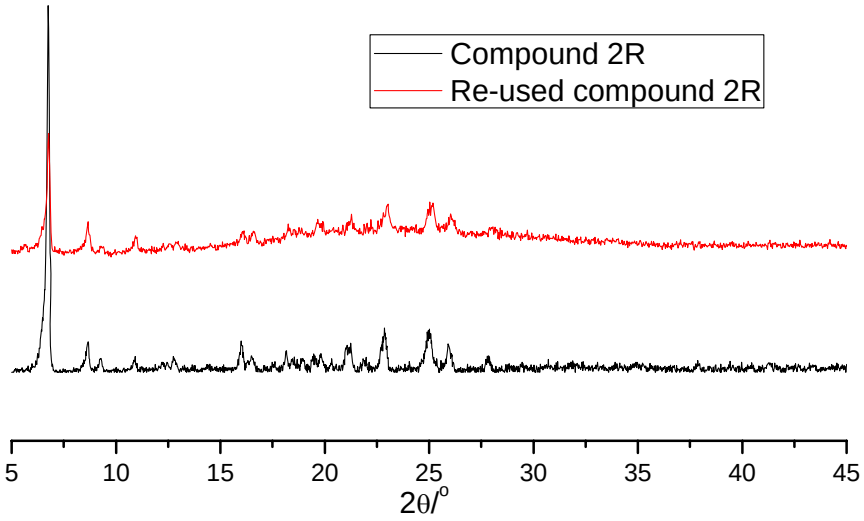

Figure S13. PXRD patterns of compound **2R** before and after the first catalysis cycle

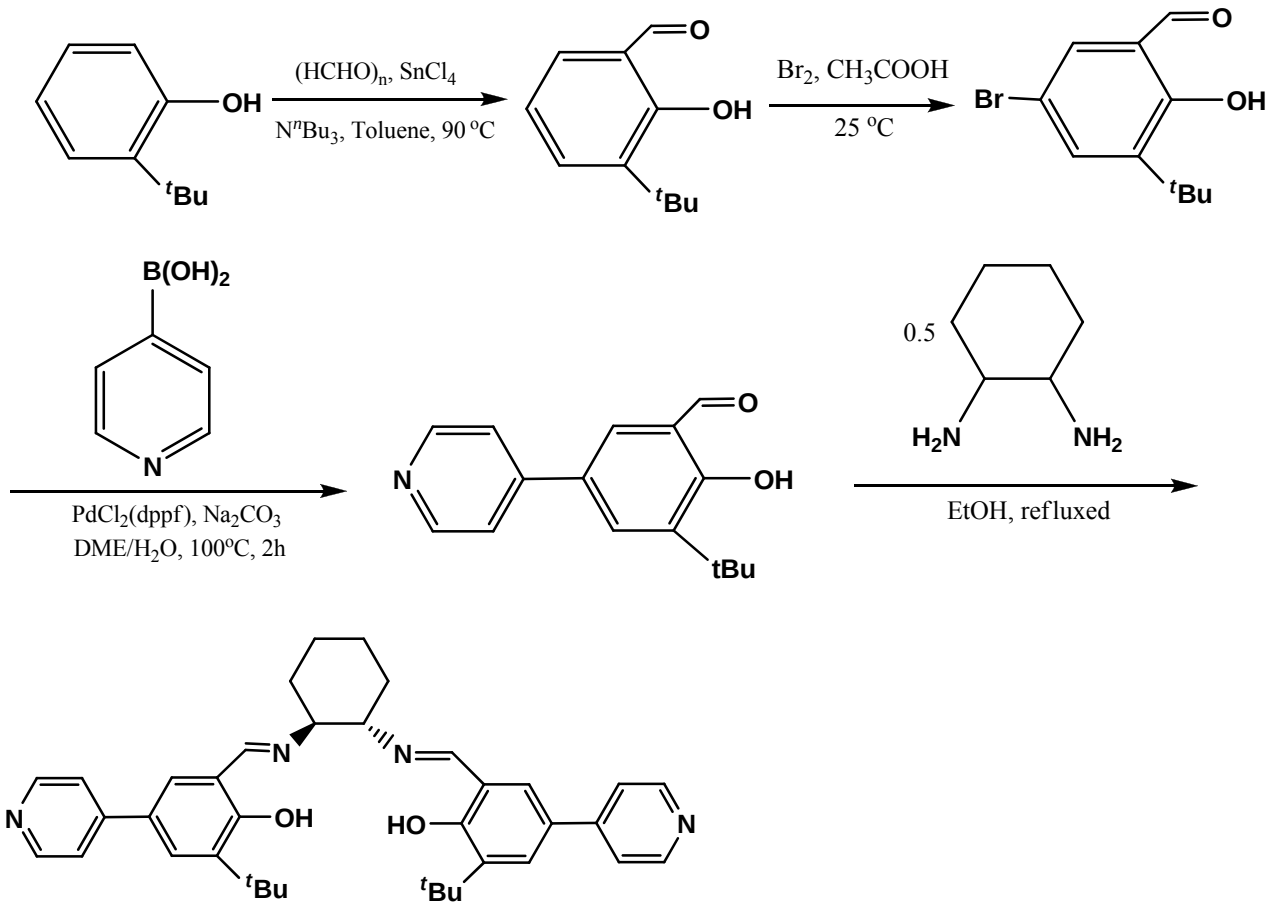

Scheme S1. Syntheses of ligand *RR*-H_2L and *SS*-H_2L

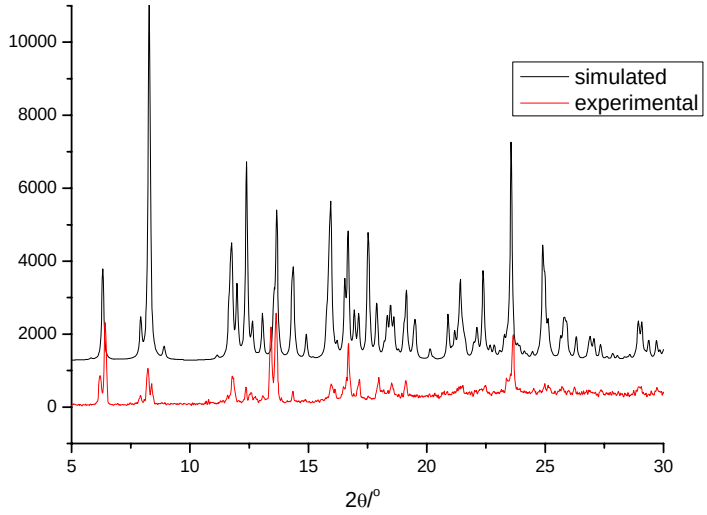

Figure S14. PXRD patterns of compound **6**